MOLECULAR AND CELLULAR BIOLOGY, May 2005, p. 4250–4261 Vol. 25, No. 10
0270-7306/05/$08.00+0 doi:10.1128/MCB.25.10.4250–4261.2005

Identification and Characterization of SSTK, a Serine/Threonine Protein Kinase Essential for Male Fertility

Nikolay A. Spiridonov,[1]* Lily Wong,[1] Patricia M. Zerfas,[2] Matthew F. Starost,[2] Svetlana D. Pack,[3] Cloud P. Paweletz,[4]† and Gibbes R. Johnson[1]*

Division of Therapeutic Proteins, Center for Drug Evaluation and Research, Food and Drug Administration, Bethesda, Maryland 20892[1]; Division of Veterinary Resources, National Institutes of Health, Bethesda, Maryland 20892[2]; Laboratory of Immunopathology, National Institute of Allergy and Infectious Diseases, National Institutes of Health, Bethesda, Maryland 20892[3]; and Uniformed Services University of the Health Sciences, Department of Anatomy, Physiology and Genetics, Institute of Molecular Medicine, Bethesda, Maryland 20814[4]

Received 26 October 2004/Returned for modification 22 November 2004/Accepted 5 February 2005

Here we describe and characterize a small serine/threonine kinase (SSTK) which consists solely of the N- and C-lobes of a protein kinase catalytic domain. SSTK protein is highly conserved among mammals, and no close homologues were found in the genomes of nonmammalian organisms. SSTK specifically interacts with HSP90-1β, HSC70, and HSP70 proteins, and this association appears to be required for SSTK kinase activity. The *SSTK* transcript was most abundant in human and mouse testes but was also detected in all human tissues tested. In the mouse testis, SSTK protein was localized to the heads of elongating spermatids. Targeted deletion of the *SSTK* gene in mice resulted in male sterility due to profound impairment in motility and morphology of spermatozoa. A defect in DNA condensation in *SSTK* null mutants occurred in elongating spermatids at a step in spermiogenesis coincident with chromatin displacement of histones by transition proteins. SSTK phosphorylated histones H1, H2A, H2AX, and H3 but not H2B or H4 or transition protein 1 in vitro. These results demonstrate that SSTK is required for proper postmeiotic chromatin remodeling and male fertility. Abnormal sperm chromatin condensation is common in sterile men, and our results may provide insight into the molecular mechanisms underlying certain human infertility disorders.

Phosphorylation of serine, threonine, and tyrosine residues in substrate targets by protein kinases is a common posttranslational protein modification in eukaryotes and provides a fundamental mechanism for the control of cellular events. Cell division and growth, adhesion and migration, metabolic activity and responses upon environmental stimuli, cell to cell communication, signal transduction, and apoptosis are among the many processes regulated by protein kinases (15, 16). At the molecular level, phosphorylation and dephosphorylation of enzymes allow fast and sensitive regulation of enzyme activity and are also a major mechanism of transmembrane signaling and signal amplification in the branching network of intracellular protein kinase cascades that ultimately control gene expression by phosphorylation of transcription factors. Phosphorylation of protein substrates can provide binding sites for protein domains which recognize specific phosphorylated amino acid sequences, thereby mediating protein-protein interactions. Protein kinases constitute a large superfamily of related enzymes which contain 12 conserved subdomains folded into N- and C-lobes of the catalytic domain. The superfamily is subdivided into protein serine/threonine kinases, protein tyrosine kinases, and atypical kinases on the basis of substrate specificity (14, 16).

Phosphorylation events play a central role in chromatin remodeling during mitosis in somatic cells and during meiosis in mammalian spermiogenesis (2, 10). Much less is known about the mechanisms of postmeiotic chromatin condensation. The structure of chromatin changes dramatically during postmeiotic spermiogenesis, as germ cells develop from round spermatids to fully differentiated spermatozoa. After the completion of meiosis, transcription ceases, and germ cells undergo complex chromatin remodeling and reconstruction of the cytoplasm. Nucleosomes are disassembled in elongated spermatids, and histones are displaced by small basic transition proteins TP1 and TP2, which are subsequently replaced with protamines. As a result of postmeiotic chromatin compaction, the haploid genome in the sperm head is highly packed within a volume of ~5% of that of a somatic nucleus, in a structure that is fundamentally different from the nucleosomal architecture of a somatic cell (20, 28). Mouse knockout studies demonstrated that the final stages of chromatin compaction are mediated by the calcium/calmodulin-dependent kinase 4 (CaMK4), which phosphorylates protamine 2 (34). However, no kinase has been implicated in the initiation and early stages of chromatin condensation.

Here we report the identification and characterization of a novel mammalian *s*mall *s*erine/*t*hreonine protein *k*inase gene, *SSTK*, which is expressed in elongating spermatids and specifically phosphorylates histones H1, H2A, H2AX, and H3. We describe human and mouse *SSTK* cDNAs, gene expression pattern, the biochemical properties of the SSTK protein, and

* Corresponding author. Mailing address: Division of Therapeutic Proteins, Center for Drug Evaluation and Research, Food and Drug Administration, HFD-122, Bldg. 29A, Rm. 3B-20, 8800 Rockville Pike, Bethesda, Maryland 20892. Phone: (301) 827-1764. Fax: (301) 480-3256. E-mail for Nikolay A. Spiridonov: spiridonov@cber.fda.gov. E-mail for Gibbes R. Johnson: johnsong@cber.fda.gov.

† Present address: Merck and Co., Inc., Molecular Profiling, Rahway, NJ 07065.

stable complex formation with heat shock proteins HSP90-1β, HSP70-1, and HSC70. We also demonstrate that a targeted deletion of *SSTK* from the mouse genome resulted in male sterility due to impaired postmeiotic chromatin condensation and abnormal spermiogenesis.

MATERIALS AND METHODS

mRNA analyses. Northern blots (Clontech) were probed with random primed ^{32}P-labeled DNA fragments corresponding to coding regions of human (1-kb AvrII/SmaI) and mouse (0.74-kb SmaI) *SSTK* cDNAs using the Strip-EZ DNA kit and hybridized in ULTRAhyb (Ambion) at 42°C for 6 h. Membranes were washed twice with 2× SSC (1× SSC is 0.15 M NaCl plus 0.015 M sodium citrate)–0.1% sodium dodecyl sulfate (SDS), three times with 0.1× SSC–0.1% SDS, and exposed to film. Total RNA was isolated using RNA-Bee (Tel-Test), and reverse transcription was carried out with Moloney murine leukemia virus reverse transcriptase and random decamer primers (Ambion). A 373-bp fragment of the human *SSTK* gene was amplified with SuperTaq DNA polymerase (Ambion) and gene-specific primers 5′-TAGGCGCCACCATGTCGGGAGAC and 5′-CCGGCGATCTGCGCAAAGAGGT.

cDNA constructs. The epitope-tagged SSTK (Myc-SSTK) expression construct was generated by PCR and subcloning into XbaI and HindIII sites of pcDNA3.1/Myc-His (Invitrogen). D145N and K41M point mutations were generated with a QuickChange kit (Stratagene). The Myc-tagged SHP-2 and GRB2 constructs have been described previously (5). The identity of all expression constructs was confirmed by DNA sequencing.

SSTK antiserum and Western blotting. Rabbit antiserum against a synthetic COOH-terminal peptide, NH_2-(K)PSAGQVARNCWLRAGDSG-COOH, of human SSTK protein was prepared. Antibodies were purified using peptide antigen immobilized on AminoLink gels (Pierce). Western blotting was performed as previously described (5). Anti-HSC70 (B-6) and anti-HSP90 α/β (H-114) antibodies were from Santa Cruz Biotech. Blots were exposed to film or quantified using Kodak 440CF image station.

Expression and immunopurification of SSTK. Transient expression of Myc-SSTK in human 293T cells was performed by transfection with Lipofectamine 2000 reagent (Gibco BRL). Stable murine 32D cells expressing Myc-SSTKs were generated using the protocol described previously (4). Cells were lysed in 20 mM HEPES, pH 7.4, 50 mM NaCl, 50 mM NaF, 5 mM EDTA, 0.1% Triton X-100, 30 mM Na pyrophosphate, 10 mM β-glycerophosphate, 1 mM Na orthovanadate, 1 mM phenylmethylsulfonyl fluoride, 2 μg/ml pepstatin A, 2 μg/ml aprotinin, and 2 μg/ml leupeptin (lysis buffer) on ice. Myc-SSTK was immunoprecipitated using 9E10 Myc antibody, and immune complexes were captured on protein G-Sepharose (Pharmacia) and washed twice with lysis buffer and once with kinase wash buffer containing 20 mM HEPES (pH 7.4), 10 mM $MgCl_2$, 2 mM EGTA, 5 mM β-glycerophosphate, 100 μM orthovanadate, and 0.5 mM dithiothreitol.

Kinase assay and phosphoamino acid analysis. Kinase reactions were performed in 20 μl of kinase wash buffer that contained 30 μM ATP, 10 μCi [γ-^{32}P]ATP, and substrate for 30 min at 25°C. Peptides and full-length murine transition protein TP1 were synthesized, purified, and characterized as previously described (9), Cdc/Cdk substrates (Santa Cruz Biotech), myelin basic protein (Sigma), calf histone H1, human recombinant histones H2A, H2A.X, H2B, and H3, and *Xenopus laevis* recombinant histone H4 (Upstate Biotech) were used as substrates. Reactions were terminated by boiling and separated on 4 to 20% SDS-polyacrylamide gel electrophoresis (PAGE) gels and transferred to membranes, and autoradiography was performed. Phosphoamino acid analysis was performed using Hunter thin-layer peptide mapping system HTLE-7000 (C.B.S. Scientific). Radiolabeled myelin basic protein (MBP) bound to polyvinylidene difluoride membrane was hydrolyzed in 6 N HCl for 1 h at 110°C and dried and hydrolysate was subjected to two-dimensional electrophoresis on thin-layer chromatography cellulose plates (Merck) as described (17). Autoradiography was performed and the positions of phosphoamino acid standards were detected with ninhydrin reagent. In some experiments reactions were terminated by acidification and phosphorylation was quantified as previously described (9).

Mass spectrometry. In-gel digestion and analysis of peptides by mass spectrometry were performed as previously described (33). Briefly, peptides were analyzed on an LCQ-DECA XP Plus ion trap mass spectrometer equipped with a nanoelectrospray source and an online Surveyor high-pressure liquid chromatograph (Thermo Finnigan) in the positive-ion mode. Proteins were identified by searching the resulting fragmentation spectra against the nonredundant Fasta database (NCBI) using Sequest. For multiple charged peptide fragments, X correlation scores above 2.5 were considered reliable.

Generation of *SSTK*$^{-/-}$ mice. The mouse *SSTK* locus was isolated from a 129 SvEv genomic DNA library and inserted into a modified pSP72 vector (Promega). A targeting vector was constructed by using an 8-kb SmaI genomic DNA fragment as the long arm. A 1.6-kb fragment located 29 bp downstream from the poly(A) signal of *SSTK* gene was PCR amplified and used as the short arm. The complete coding sequence of the *SSTK* gene (8 bp of 5′ untranslated region to 401 bp of 3′ untranslated region) was replaced with a neomycin resistance cassette flanked with *loxP* sites. The targeting construct was linearized and electroporated into 129 embryonic stem (ES) cells. After selection in G418, surviving colonies were expanded and PCR analysis was performed to identify clones that had undergone homologous recombination. PCR was performed using primers S1 (5′-TGCGAGGCCAGAGGCCACTTGTGTAGC) and A1 (5′-ACCATAGGCTATGGGCTCGAGCAG), and S2 (5′-GGGGCAGGTTCCGCTTGTAGTCG) and A2 (5′-GGCCAGCTCATTCCTCCCACTCAT), and the products were sequenced (Fig. 5A).

ES cells were microinjected into C57BL/6 mice embryos and implanted into pseudo-pregnant females. Chimeric mice were mated with C57BL/6 mice and heterozygotes were intercrossed to produce homozygous offspring. Transmission of the targeted allele was verified by PCR using primers S3 (5′-CGAGCGCCTCCGGACTTCGTCAAC) and A3 (5′-CGCCGGGGTAGGCCAGCAATGTC) for the wild type, and S2 and A2 for the knockout allele. The animals were housed under specific-pathogen-free conditions on a 12h–:12-h light-dark cycle with ad libitum access to food and water. All protocols were in accordance with National Institutes of Health guidelines and were approved by Animal Care and Use Committee of the National Institutes of Health.

Immunohistochemistry. Testicular tissues were fixed in 10% formalin, dehydrated, and paraffin embedded. SSTK was detected using 5 μg/ml affinity-purified antibodies and the Vector ABC Elite kit (Vector Laboratories). Sections were counterstained with hematoxylin.

In situ hybridization. Tissue sections were fixed in 4% paraformaldehyde and dehydrated in cold (−20°C) ethanol for 2 min. A DNA probe derived from the *SSTK* coding sequence was generated by PCR with biotin-16-dUTP, precipitated, and dissolved in hybridization solution (50% formamide, 10% dextran sulfate, 2× SSC). After hybridization with denatured probe, slides were washed three times in a 50% formamide/2× SSC mixture at 45°C, twice in 1× SSC, and twice in 0.1× SSC. Bound probe was detected with 5 μg/ml fluorescein isothiocyanate conjugated to avidin (Vector Laboratories). Slides were counterstained with propidium iodide, and images were acquired on a Zeiss Axiophot-2 fluorescence microscope (Carl Zeiss) using a Photometrics charge-coupled device camera (Photometrics) and IPLab Spectrum software (Scanalytics).

Mating experiments and sperm analysis. Two- to 6-month-old male *SSTK*$^{-/-}$ mice and their *SSTK*$^{+/-}$ littermates were crossed with wild-type or *SSTK*$^{+/-}$ females. To establish infertility, every male was successively bred to several fertile females, for at least 2 weeks each. Sperm analysis was performed by Charles River Laboratories. Briefly, the epididymis was isolated and sperm was released into 125 μl of human tubal fluid (Conception Technologies) supplemented with 0.4% bovine serum albumin. The sperm was analyzed at 37°C utilizing the Hamilton Thorne Biosciences IVOS System, version 12.2.

Electron microscopy. Testes, epididymis tissue, and sperm were fixed in 2.5% glutaraldehyde in 0.1 M cacodylate buffer, pH 7.4, overnight. All tissues were washed with buffer, fixed with 1% osmium tetroxide for 2 h, washed with buffer, serially dehydrated in ethanol and propylene oxide, and embedded in Eponate 12 resin (Ted Pella). Sections (~80 nm) were obtained with an Ultracut-UCT ultramicrotome (Leica), placed onto 400-mesh copper grids, and stained with saturated uranyl acetate in 50% methanol followed by lead citrate. Grids were viewed in a Philips 410 electron microscope (FEI) at 80 kV, and images were recorded on Kodak SO-163 film.

Nucleotide sequence accession numbers. The cDNA sequences for human and mouse SSTK have been deposited in GenBank with accession numbers AF329483 and AF329484, respectively.

RESULTS

Identification and structure of human and mouse *SSTK* genes. We predicted the *SSTK* gene using the BLAST program (1) in the unfinished draft of the human chromosome 19 on the basis of sequence homologies to a protein kinase catalytic domain. A murine orthologue of the *SSTK* gene was found in the mouse genome draft and later mapped to chromosome 8 by aligning with the mouse draft genome assembly (http://www.genome.ucsc.edu). Candidate human and murine cDNA

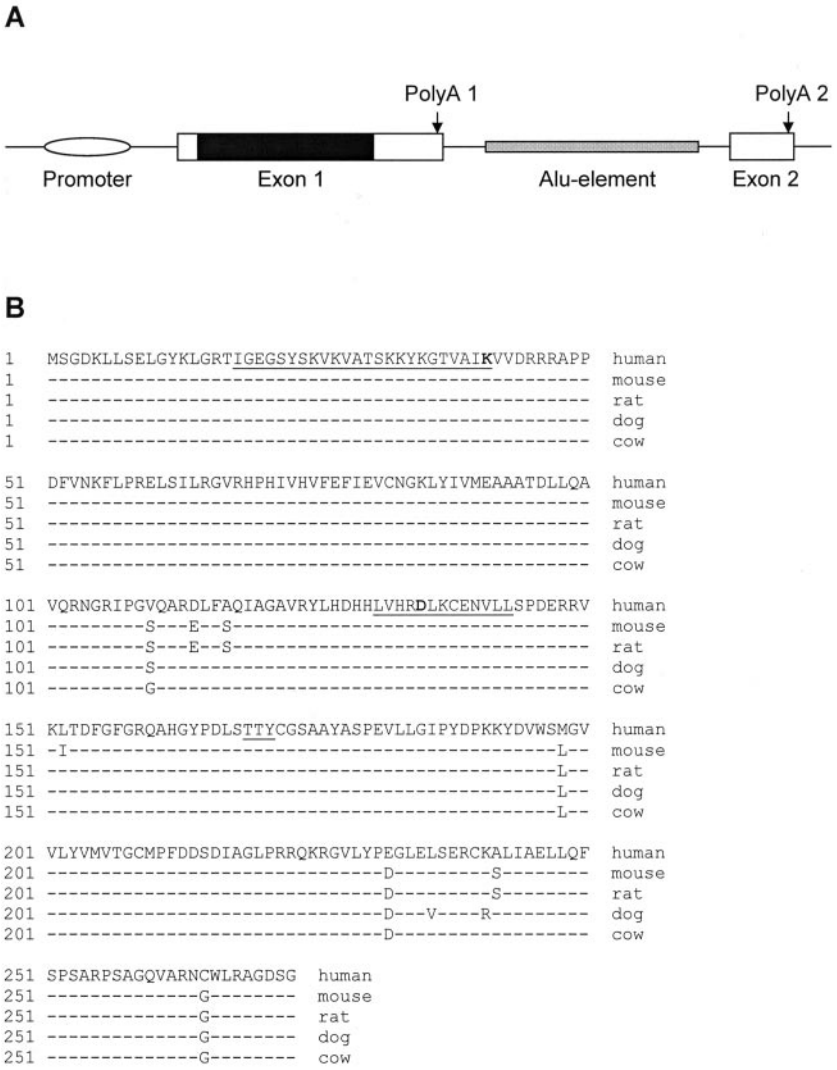

FIG. 1. Structure of the human *SSTK* gene and alignment of mammalian SSTK proteins. A. Structure of the human *SSTK* gene. The schematic represents relative positions and is not drawn to scale. The nucleotide positions of features shown relative to the translation start codon are as follows: promoter, −294 to −123; exon 1, −122 to 1273; protein coding sequence (solid), 1 to 822; poly(A) 1, 1188 to 1193; Alu element, 1604 to 2700; exon 2, 2886 to 3007; poly(A) 2, 2990 to 2995. B. Alignment of human (AF329483), mouse (AF329484), rat (XM_224740), dog (AAEX01022953), and cow (AAFC01290160) SSTK proteins. Conserved protein kinase active site (amino acids 131 to 143), ATP-binding region (amino acids 18 to 41), and potential activation loop phosphorylation motif (amino acids 169 to 171) are underlined. Conserved catalytic (D135) and ATP-binding (K41) residues are boldfaced.

clones were identified in expressed sequence tag (EST) databases by homology searches to their 3′ untranslated regions, obtained, and sequenced. The complete coding sequences of both strands of the human and mouse *SSTK* cDNAs were determined and submitted to GenBank with accession numbers AF329483 (human) and AF329484 (mouse) in December 2000. The sequences of the human and murine *SSTK* genes are highly conserved, with 90% identity in the DNA coding region.

Alignment of the human *SSTK* cDNA with genomic DNA showed that the last 125 bases of the 3′-terminal region of the human transcript were located on the second nontranslated exon, and splicing occurred on conserved donor and acceptor splicing sites. A 1,612-nucleotide intron between the two exons contained an Alu element (Fig. 1A). Analysis of ESTs in GenBank provided evidence for the existence of three splicing isoforms of the human mRNA that were polyadenylated at two different sites. Eight sequences (AA608857, AA913074, AI024234, AI025487, AI150036, AI827749, AW662022, and BC014611) represent a 1.35-kb transcript that is polyadenylated at poly(A) site 1. AF329483 and BI828962 represent a ~1.5-kb isoform that is polyadenylated at poly(A) site 2, spliced, and possessed the second nontranslated exon. Three ESTs (CN315260, CN263467, and BF972639) correspond to a longer (~3-kb) isoform polyadenylated at poly(A) site 2 without splicing. No evidence for alternative splicing of the mouse *SSTK* gene was found.

Amino acid sequence of SSTK. Both the human and mouse transcripts encode a 273-amino-acid residue protein with calculated molecular mass of ~30.3 kDa and an isoelectric point of ~9.1. SSTK protein sequences from human, mouse, rat,

dog, and cow revealed a highly conserved structure, with 97 to 98% identity (Fig. 1B). No close homologies were found in the genomes of nonmammalian organisms. Phylogenetic analysis placed SSTK among the members of the CaMK group (data not shown). SSTK shows moderate similarity to mammalian testis-specific serine/threonine kinases TSSK1, TSSK2, and TSSK3 (45 to 49% identity), mitogen-activated protein kinase/microtubule affinity-regulating kinases MARK and MARK4, and the ELKL motif kinase EMK1 (38 to 39% identity).

The SSTK protein consists almost entirely of the N- and C-lobes of a protein kinase domain (amino acids 13 to 268). SSTK possesses essential protein kinase features, including conserved catalytic and ATP-binding regions, the indispensable catalytic residues K41, E60, D135, N140, D154, and T170, a glycine-rich sequence motif (amino acids 19 to 24) in the phosphate-binding loop, and the conserved DFG sequence (amino acids 154 to 156) within the active site (18). SSTK contains characteristic tyrosine phosphorylation motifs (K/R-X-X-X-E-X-X-Y) near its NH_2 terminus (amino acids 5 to 12 and 16 to 23) which are homologous to the NH_2-terminal inhibitory phosphorylation sites in human cyclin-dependent kinases Cdc2 and Cdk2 (12). SSTK contains a TTY sequence (amino acids 169 to 171) which is homologous to the T-X-Y phosphorylation motif found in the activation loop of the mitogen-activated protein kinases (MAPKs) (3). In addition, SSTK possesses a sequence (amino acids 217 to 225) that is similar to the characteristic MAPK insert located between subdomains X and XI. This sequence in SSTK is most similar to the insert of ERK2 relative to other members of the MAPK family (14).

In vivo expression pattern of *SSTK*. The in vivo expression of the *SSTK* gene was studied by Northern blot analysis of poly(A)-selected mRNA, and reverse transcription (RT)-PCR analysis of total RNA from human organs. Abundant expression of a single transcript (~1.5 kb), whose size was consistent with *SSTK* cDNA, was detected in the adult human testis (Fig. 2A, lane 4). A lower level of expression was also detected in human colon, small intestine, ovary, prostate, thymus, spleen, and peripheral blood leukocytes in a longer exposure of the blot to film (Fig. 2A, lower panel). SSTK transcript was also detected in human testis mRNA by RT-PCR analysis after 30 cycles of amplification (Fig. 2B, lane 5), whereas amplification for 35 cycles was necessary to detect message in kidney, liver, skeletal muscle, colon, and prostate (Fig. 2B, lower panel). The identity of the RT-PCR products derived from the testis, kidney, liver, and prostate was confirmed by restriction analysis (data not shown).

Northern blot analysis of mRNAs purified from various human brain structures detected a ~3-kb transcript in the spinal cord and medulla oblongata (Fig. 2C). The size of this longer mRNA is consistent with the expected size of a transcript polyadenylated at poly(A) site 2 without splicing. Northern blot analysis of poly(A)-enriched RNA from murine testis identified a ~1.4-kb *SSTK* transcript (Fig. 2D, lane 1), which was in good agreement with the size of the mouse cDNA.

Taken together, Northern blotting and RT-PCR results are consistent with the occurrence of ESTs to the *SSTK* gene in the human database that originate mostly from the testis (14 EST sequences) but also from other organs and tissues such as kidney, embryonic stem cells (two EST sequences), breast,

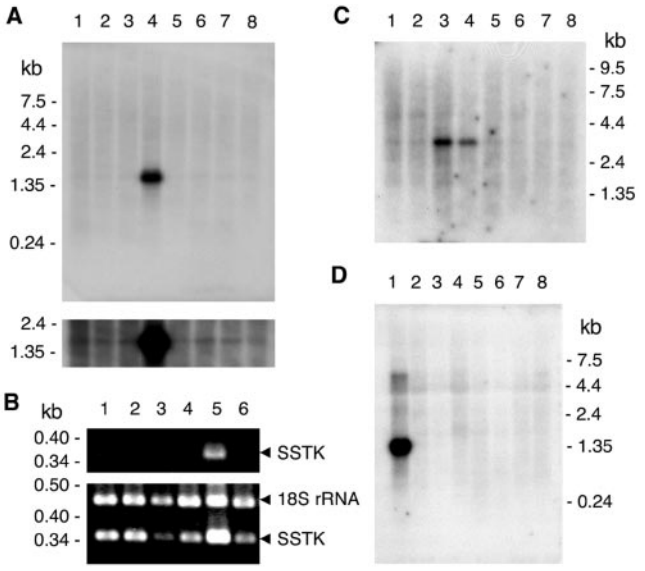

FIG. 2. In vivo expression of SSTK. A. Northern blot analysis of *SSTK* mRNA in human organs. The human multiple tissue blot was probed with the ^{32}P-labeled *SSTK* DNA probe under stringent conditions as described in the text and exposed to film for 20 h at 4°C (top) and −70°C (bottom). The positions and sizes of markers are indicated in kilobases. The samples in lanes 1 to 8 correspond to spleen, thymus, prostate, testis, ovary, small intestine, colon, and peripheral blood leukocytes, respectively. B. Competitive RT-PCR analysis of *SSTK* mRNA in human organs. Total RNA was reverse transcribed and amplified using SSTK primers yielding a 373-bp product. No products were observed without reverse transcription. 18S rRNA primers and competimers were used in same reaction to amplify a 489-bp 18S rRNA internal control product (Ambion). Amplification was performed for 30 (top) or 35 (bottom) cycles. Products were separated on agarose gels and stained with ethidium bromide. The samples in lanes 1 to 6 correspond to kidney, liver, skeletal muscle, colon, testis, and prostate, respectively. Products are denoted on the right. C. Analysis of human brain tissues. The multiple-tissue Northern blot was probed and exposed to Kodak film for 24 h at −70°C. The mRNA samples in lanes 1 to 8 correspond to cerebellum, cerebral cortex, medulla oblongata, spinal cord, occipital pole, frontal lobe, temporal lobe, and putamen, respectively. D. Analysis of mouse organs. The Northern blot was probed with the ^{32}P-labeled *SSTK* DNA probe and exposed to film for 20 h at 4°C. The mRNA samples in lanes 1 to 8 correspond to testis, kidney, skeletal muscle, liver, lung, spleen, brain, and heart, respectively.

pancreas, brain medulla, fetal liver and spleen, uterus, B-cell leukemia, lung carcinoma, uterus leiomyosarcoma, and ovary fibrotheoma (one each). Similarly, ESTs to the mouse *SSTK* gene originated mostly from the testis (16 sequences) but also from cerebellum, thymus, branchial arches, and placenta (one each).

Biochemical characterization of SSTK. For evaluation of enzyme activity, Myc epitope-tagged wild-type and mutant versions of human SSTK were expressed in 293T cells, immunopurified with Myc antibodies, and subjected to in vitro kinase assays using myelin basic protein (MBP), a substrate commonly used in MAPK kinase assays. Myc-SSTK phosphorylated MBP, as demonstrated by the transfer of radiolabel from [^{32}P]ATP into MBP (Fig. 3A). To confirm that the protein kinase activity was intrinsic to SSTK, we performed experiments with kinase-inactive SSTKs in which the predicted active-site residue D135 and ATP-binding residue K41 were replaced with nonfunctional amino acid residues. The K41M and

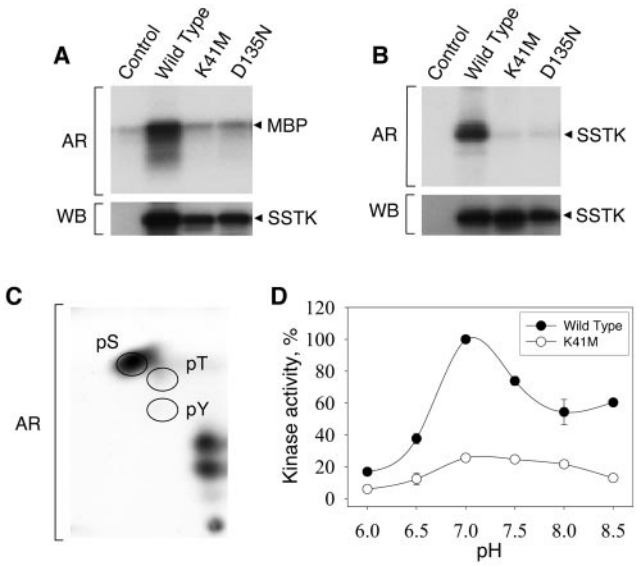

FIG. 3. Characterization of SSTK kinase activity. A. 293T cells were transfected with empty vector (control) or constructs expressing wild-type, K41M, or D135N Myc epitope-tagged SSTKs, lysates were generated, and immunoprecipitations were performed using Myc 9E10 monoclonal antibody as described in the text. Immunoprecipitates were subjected to in vitro kinase reactions containing [^{32}P]ATP and 1 μg/μl myelin basic protein for 30 min at 25°C (MBP). Reaction mixtures were fractionated in a 4 to 20% SDS-PAGE gel, transferred to PVDF membrane, and autoradiography (AR) and Western blotting (WB) using SSTK antiserum were performed. B. SSTKs were expressed and immunopurified as above. Kinase reactions were performed using [^{32}P]ATP alone. C. Phosphoamino acid analysis was performed on MBP phosphorylated by Myc-SSTK using [^{32}P]ATP. MBP bound to polyvinylidene difluoride membrane was hydrolyzed and subjected to two-dimensional electrophoresis followed by autoradiography. The migratory positions for phosphoserine (pS), phosphothreonine (pT), and phosphotyrosine (pY) have been denoted with circles. Autoradiography exposure times in panels A, B, and C were 0.3, 30, and 48 h, respectively. D. Effect of pH on SSTK kinase activity. SSTKs were immunoprecipitated and subjected to kinase reactions as in A at the indicated pH. ^{32}P incorporation into MBP was quantified as previously described (9). Data represent mean ± standard error of the mean (n = 3).

D135N mutations in Myc-SSTK decreased phosphorylation of MBP to the level observed in the empty vector control (Fig. 3A). Analogous experiments performed in the absence of exogenous protein substrate revealed SSTK autokinase activity, as evidenced by the incorporation of radiolabel into a protein with a molecular mass of ~33 kDa that was recognized by SSTK antiserum in Western blotting (Fig. 3B). These findings demonstrate that SSTK possesses intrinsic protein kinase activity and can utilize MBP as well as itself (autokinase) as substrates.

Phosphoamino acid analysis of MBP phosphorylated by Myc-SSTK demonstrated that phosphorylation occurred almost entirely on serine residues (Fig. 3C). A small amount of phosphorylation on threonine residues was also observed in extended autoradiography (data not shown). No significant radiolabeled phosphoamino acid was generated from reactions performed using K41M Myc-SSTK (data not shown). These results provide evidence that SSTK belongs to the serine/threonine family of protein kinases. An analysis of SSTK kinase activity towards the MBP substrate at pH values ranging from 6.0 to 8.5 demonstrated the enzyme had a pH optimum of 7.0 under these conditions (Fig. 3D). To test the effects of various stimuli on SSTK kinase activity, 293T cells were transfected with Myc-SSTK cDNAs, serum starved overnight, and treated with either 2 nM of epidermal growth factor for 4 min, or 10% fetal bovine serum, 50 nM phorbol 12-myristate 13-acetate, 2 μM of forskolin, or 50 μM of 3-isobutyl-1-methylxanthine for 20 min. SSTK was immunopurified and kinase reactions were performed using MBP as a substrate. Neither epidermal growth factor, fetal bovine serum, or phorbol 12-myristate 13-acetate had any significant effect on SSTK kinase activity, whereas forskolin and 3-isobutyl-1-methylxanthine led to a modest ~40% decrease in activity, suggesting that SSTK enzymatic activity may be affected by cellular cyclic AMP levels (data not shown).

SSTK forms stable complexes with HSP90-1β, HSC70, and HSP70-1. Since SSTK appeared to be composed solely of a kinase catalytic domain, we believed that SSTK may represent a subunit of a larger protein complex. To detect cellular proteins which interact with SSTK, we used a coimmunoprecipitation approach. 293T cells were transfected with plasmids encoding wild-type or K41M Myc-SSTK. Cells were lysed, Myc-SSTKs were immunoprecipitated, and immune complexes were analyzed by SDS-PAGE and silver staining. As shown in Fig. 4A (left panel), one protein band of ~90 kDa and two of ~70 kDa were specifically coimmunoprecipitated with both wild-type and K41M Myc-SSTKs. These bands were not observed in immunoprecipitates from cells transfected with empty vector (control). Kinase assays using [^{32}P]ATP were carried out to determine whether the associated proteins could be phosphorylated by SSTK. No significant phosphorylation of the three protein bands was detected (Fig. 4A, right panel).

To identify the proteins which coimmunoprecipitated with SSTK, the bands were excised from the gel, digested with trypsin, and analyzed by tandem mass spectrometry. Based on the fragmentation of the resulting peptides the ~90-kDa protein was identified as HSP90 protein 1β (gi306891). The predominant ~70-kDa protein was identified as heat shock cognate protein HSC70 (gi5729877), whereas the second ~70-kDa protein was identified as HSP70 protein 1 (gi462325). A summary of the parameters used for protein identification is presented in Table 1.

To confirm that association of these heat shock proteins with SSTK is specific and not due to an interaction with the Myc or hexahistidine epitope tags or to relatively high expression in 293T cells, coimmunoprecipitation experiments were performed using several proteins expressed from the same vector and containing the identical epitope tags at the C terminus (Fig. 4B). The control proteins used to demonstrate this specificity were full-length and truncated versions of the adapter protein GRB2 and protein tyrosine phosphatase SHP-2 (lanes 4 to 10). The three heat shock proteins bound to Myc-SSTK were not observed in silver-stained gels containing immunoprecipitates from cells expressing Myc-GRB2 or Myc-SHP-2. Further, no HSP90 or HSC70 was detected by Western blotting in immunoprecipitates from cells transfected with empty vector or GRB2/SHP-2 cDNAs (Fig. 4B, lower panels, lanes 1 and 4 to 10), but was easily detected in the Myc-SSTK samples (Fig. 4B, lanes 2 to 3). Taken together, these results indicate

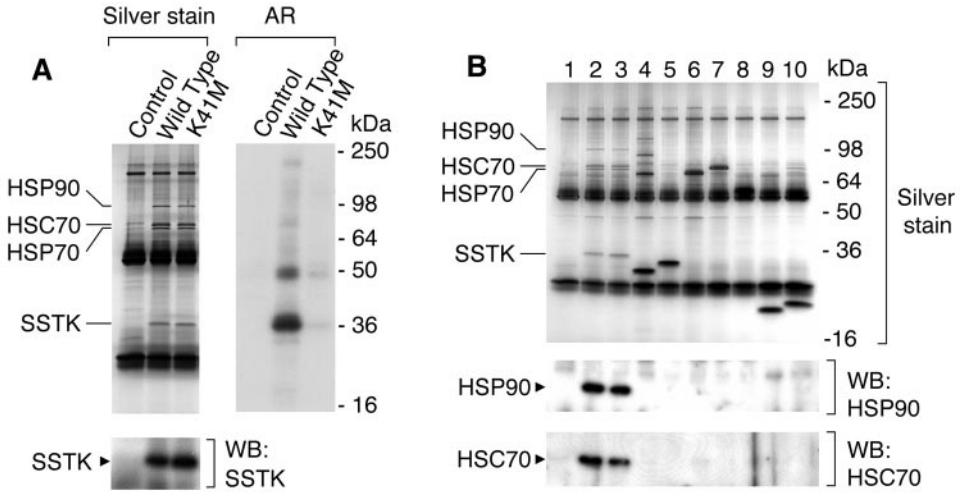

FIG. 4. Detection and analysis of proteins that associate with SSTK. A. Wild-type and K41M Myc-SSTKs were expressed in 293T cells and immunoprecipitates were analyzed by SDS-PAGE and silver staining (left panel). Western blotting (WB) was performed with SSTK antiserum. The positions of Myc-SSTK, HSP90, HSC70, and HSP70 are indicated. Intense ~25- and ~55-kDa bands are heavy and light chains of 9E10 antibody, respectively. Immunoprecipitates were subjected to kinase reactions with [^{32}P]ATP alone and subsequent autoradiography (AR). B. Confirmation of specificity of SSTK-HSP complex formation. Various cDNA constructs were transfected into 293T cells and anti-Myc immunoprecipitates were generated. All proteins contained a Myc and hexahistidine tag at the COOH terminus and were expressed in pcDNA3.1Myc/His. Immunoprecipitates were analyzed by SDS-PAGE and silver staining (upper panel) and Western blotting using antibodies against HSP90 (middle panel) and HSC70 (lower panel). The expressed proteins were: lane 1, none (vector); lane 2, SSTK; lane 3, K41M SSTK; lane 4, GRB2; lane 5, SHP-$2_{1\text{-}244}$; lane 6, SHP-$2_{110\text{-}594}$; lane 7, SHP-2; lane 8, SHP-$2_{188\text{-}591}$; lane 9, $GRB2_{1\text{-}158}$; lane 10, $GRB2_{54\text{-}217}$. Positions of Myc-SSTK, HSP90, HSC70, and HSP70 are indicated.

that SSTK specifically forms stable complexes with HSP90 and HSC70.

Catalytic specificity of SSTK. To further our studies, we generated stable 32D suspension cell lines expressing wild-type or K41M Myc-SSTKs as a source of enzyme. Consistent with our findings in 293T cells, Myc-SSTKs from 32D cells also associated with the heat shock proteins (data not shown). To evaluate preferred sequences surrounding the phosphoacceptor Ser/Thr in substrates, we measured SSTK enzymatic activity using a panel of in-house and commercially available synthetic peptides (Table 2). Peptides 1 and 5 are derived from MBP, 2 is from SSTK (residues 57 to 68), 4, 8, 9, and 10 are Cdc/Cdk substrates, and 6, 7, and 11 contain Pro at the +1 position (a specificity common to MAPKs). Peptides 3 and 12 were randomly selected. SSTK was found to phosphorylate both Ser- and, to a lower degree, Thr-containing peptides. The most pronounced phosphorylation was observed on peptides 1 and 2, which contained a common R-X-X-S-X-X-R sequence. SSTK did not significantly phosphorylate proline-directed MAPK-like substrates or Cdc/Cdk substrates.

Male infertility and sperm abnormalities in SSTK null mice. To study the biological role of SSTK in vivo, we gener-

TABLE 1. Mass spectrometric identification of proteins that form stable complexes with SSTK[a]

Protein	Peptide sequence	Ion parameters		
		m	X corr	Ions
HSP90-1β	K.VILHLKEDQTEYLEER.R	2016.29	4.005	28/60
	K.HLEINPDHPIVETLR.Q	1784.02	3.514	29/56
	K.SLTNDWEDHLAVK.H	1528.66	2.739	16/24
	K.HFSVEGQLEFR.A	1349.49	2.366	16/20
HSC70	K.NQVAMNPTNTVFDAK.R	1666.84	5.188	22/28
	K.SQIHDIVLVGGSTR.I	1482.68	3.791	18/26
	K.LNDLEEALQQAK.E	1372.52	3.684	16/22
	K.HWPFMVVNDAGRPK.V	1670.93	3.491	24/52
	R.MVNHFIAEFK.R	1252.47	3.021	18/36
	K.VQQTVQDLFGR.A	1291.45	3.562	17/20
HSP70-1	K.NQVALNPQNTVFDAK.R	1659.84	4.707	23/28
	K.AQIHDLVLVGGSTR.I	1466.68	3.089	21/52
	R.LVNHFVEEFK.R	1262.45	2.995	20/36
	K.NALESYAFNMK.S	1304.46	2.584	20/30
	K.DAGVIAGLNVLR.I	1198.41	1.921	14/22

[a] Sequences and molecular masses of identified products of tryptic digestions (m), corresponding X correlation scores (X corr), and number of ions matched used to validate protein identifications (ions) are shown. Periods within sequences represent tryptic cleavage sites.

TABLE 2. Phosphorylation of synthetic peptides by SSTK in vitro[a]

Peptide no.	Sequence	Mean phosphorylation (% of peptide 1 phosphorylation ± SEM) (n = 3)
1	GKGRGL**S**LARFAKK	100.0 ± 3.5
2	KLPREL**S**ILRGVRK	17.2 ± 1.5
3	KMERHT**S**HPNRKK	8.6 ± 0.2
4	EGVP**ST**AIREI**S**LLKE	5.7 ± 0.8
5	GGRD**S**R**S**G**S**PMARR	3.5 ± 1.0
6	KKGGAVENPEYL**T**PQGGAAK	6.6 ± 0.2
7	KKRGELDEEGYM**T**PMRDKPK	4.5 ± 0.4
8	HA**T**PPKKKRK	8.1 ± 0.4
9	PK**T**PKKAKKL	5.1 ± 5.0
10	QLQLQAA**S**NFK**S**PVK**T**IR	2.5 ± 2.5
11	KKL**T**C**S**PQPEYVNQPDVRPK	2.0 ± 1.0
12	KKKIG**T**AEPDYGALYEGRNK	0

[a] Myc-SSTK was immunopurified from stable 32D cells and kinase assays using 0.5 mM peptide were performed as described in Materials and Methods. Phosphoacceptor residues are shown in bold type. Phosphorylation by SSTK was confirmed using K41M SSTK.

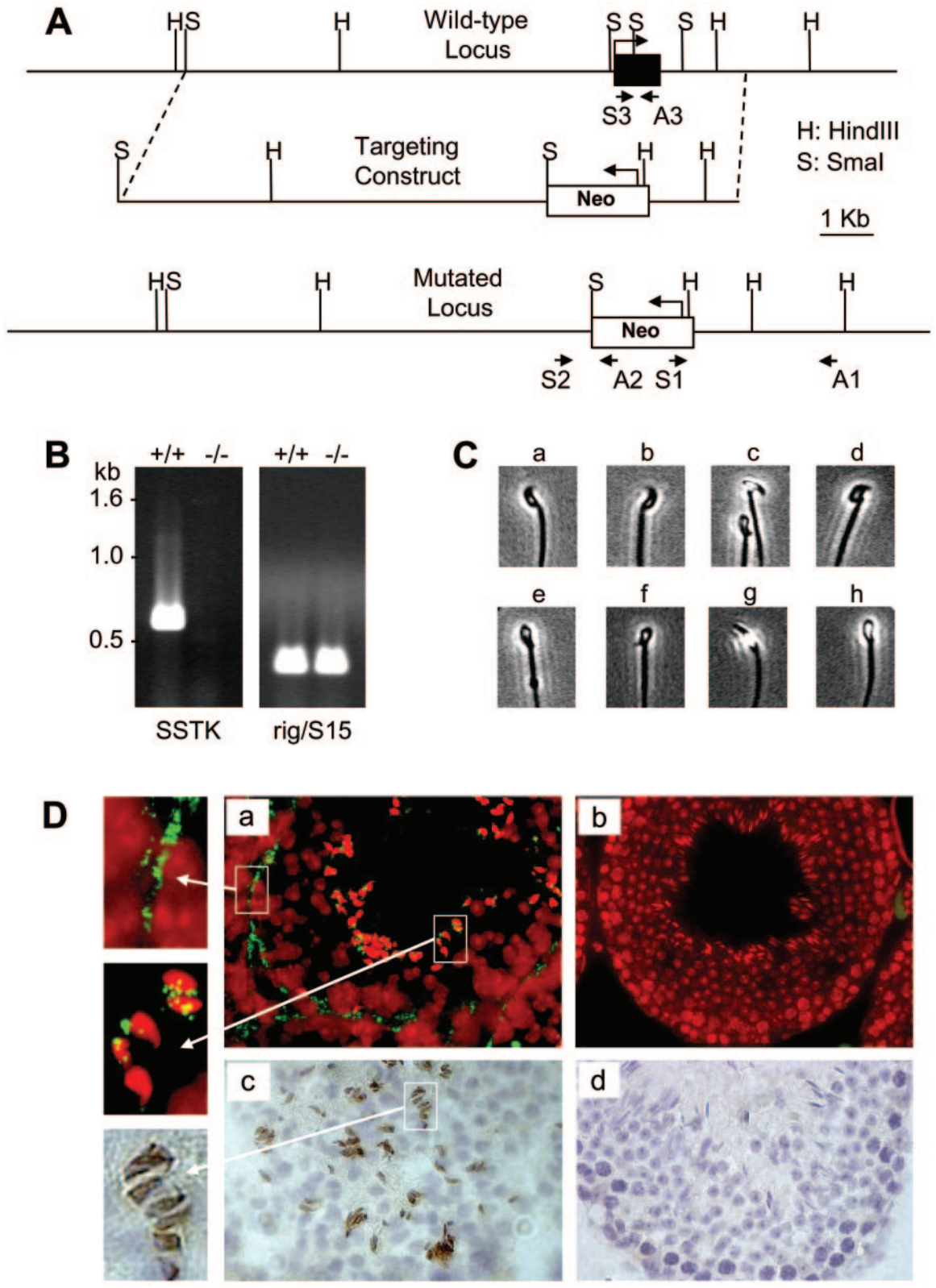

FIG. 5. Generation of mice bearing a targeted deletion of the *SSTK* gene and SSTK expression in mouse testes. A. Schematic representation of the wild-type (WT) SSTK locus, homologous recombination of targeting vector, and the mutated locus. Positions of PCR primers used for verification of homologous recombination and genotyping are indicated with arrows. B. Analysis of *SSTK* mRNA expression. RT-PCR was performed using primers S3 and A3 on RNA derived from wild-type (+/+) and *SSTK* null (−/−; left) mice. Ribosomal rig/S15 gene primers (Ambion) were used as controls (right). C. Abnormal sperm head morphology in *SSTK* null mice. Wild-type spermatozoa (a and b). Abnormal spermatozoa from *SSTK* null mice with degenerating heads (c to h). D. In situ hybridization (a and b) and immunohistochemistry (c and d)

ated SSTK knockout mice, where the complete coding sequence of the *SSTK* gene was deleted from the mouse genome (Fig. 5A). Homologous recombination and *SSTK* deletion from the mouse genomic DNA was verified by PCR and sequencing. Mice homozygous for the *SSTK* deletion were bred by mating heterozygous mutants. To confirm the absence of *SSTK* expression in $SSTK^{-/-}$ mice, we performed RT-PCR analysis of testicular RNA, immunohistochemistry, and in situ hybridization analyses of testicular tissue. As shown in Fig. 5B and D, no *SSTK* transcripts and no SSTK protein were detected in the testes of $SSTK^{-/-}$ homozygotes, confirming the null mutation.

$SSTK^{-/-}$ females were fertile, whereas $SSTK^{-/-}$ males were found to be sterile, although they were sexually active and produced vaginal plugs in female partners. To evaluate the impact of *SSTK* deletion on the structure and function of the male reproductive system, we performed histomorphology, immunohistochemistry, and in situ hybridization analyses. Mice appeared to be normal at the anatomical level. No significant differences were apparent with regard to histomorphology of the reproductive system, weight of testis and epididymis among the age-matched adult male $SSTK^{+/+}$ or $SSTK^{-/-}$ littermates (data not shown). Specific hybridization of an *SSTK* DNA probe was observed in elongating spermatids of the inner luminal cell layer of the seminiferous tubules and in spindle-shaped fibromyocytes of the lamina propria (Fig. 5D, panel a). Immunohistochemical staining with affinity-purified SSTK antibodies was observed in the heads of elongating spermatids (Fig. 5D, panel c) and in the fibromyocytes (data not shown). No immunostaining or RNA hybridization was detected in testicular sections from $SSTK^{-/-}$ mice (Fig. 5D, panels b and d).

To determine the basis for male infertility in $SSTK^{-/-}$ mice, sperm were obtained from the cauda epididymis and studied in vitro. As shown in Table 3, there was a considerable reduction in sperm counts in null mutants and heterozygotes compared to wild-type mice. Complete loss of the *SSTK* alleles resulted in a decrease in the percentage of motile sperm and motility rates and a dramatic increase in the percentage of sperm with abnormal morphology. The most common abnormalities found in $SSTK^{-/-}$ spermatozoa were associated with head morphology, such as a failure to develop hook-shaped heads, irregular-shaped and degenerate heads, and improper attachment of the midpiece (Fig. 5C).

The morphology of testicular tissue, epididymis, and mature sperm from $SSTK^{-/-}$ relative to wild-type mice was studied by electron microscopy. The earliest morphological defects were detected in the heads of step 10 SSTK null elongating spermatids that displayed characteristic enlargement of the space between the nuclear envelope and condensing nucleus of the posterior head (Fig. 6 a to c). Further expansion of the perinuclear and subacrosomal space and accumulation of electron-dense matter between the membranes of the head and nucleus were observed in step 12 SSTK null elongating spermatids (Fig. 6 d to f). These morphology defects were also prominent in maturing sperm of the epididymis (data not shown) and in mature sperm heads (Fig. 6 g to i). No apparent abnormalities were found in the acrosome, midpiece, or sperm flagellum. Propidium iodide staining of epididymal sperm from SSTK knockout mice demonstrated reduced DNA compaction in the heads of SSTK null spermatozoa compared to wild-type mice (Fig. 7). These findings confirmed the significant impairment of DNA condensation in SSTK knockout spermatozoa.

TABLE 3. Impaired sperm morphology and motility in *SSTK* null mice

Parameter	Wild type	$SSTK^{+/-}$	$SSTK^{-/-}$
Sperm count (10^6/ml)	216.5 ± 10.9	107.0 ± 5.9	95.3 ± 13.3
Motile spermatozoa (%)	60.5 ± 4.1	69.7 ± 6.3	29.0 ± 6.3
Rapid spermatozoa[a] (%)	52.8 ± 4.8	64.0 ± 6.6	17.0 ± 5.7
Normal morphology (%)	51.5 ± 3.0	42.0 ± 4.2	2.3 ± 1.2
Abnormal head (%)	16.0 ± 3.3	16.0 ± 0.6	90.3 ± 5.1

[a] Cells moving in a straight path with a velocity greater than 50 μm per second. Data represent mean ± SEM, $n = 3$.

The observed deficiency in DNA condensation in SSTK null elongating spermatids temporally coincided with chromatin remodeling and displacement of testis-specific and somatic histones by transition proteins (reviewed in reference 20). For this reason and the in vitro preference of SSTK for phosphorylation of Ser sites within a basic context, we tested the hypothesis that histones may be substrates for SSTK. Importantly, in vitro SSTK phosphorylated histones H1, H2A, H2AX, and H3 but not H2B, H4, or TP1 (Fig. 8). No phosphorylation was observed using the control kinase-inactive SSTK.

DISCUSSION

SSTK is a serine/threonine protein kinase. SSTK is one of the smallest protein kinases and is composed of the minimum structure necessary to impart intrinsic protein kinase catalytic function to a polypeptide. The high degree of conservation of SSTK between the human, mouse, rat, dog, and cow, together with the absence of close homologues in fish, worm, and insect complete genomes, suggests a late evolutionary origin for this gene and its restriction to higher vertebrates or mammals. Although the *SSTK* gene is abundantly expressed in the adult testis and our results demonstrate a requisite role for SSTK in spermiogenesis, the ubiquitous expression pattern and the fact that transcripts of the human and murine *SSTK* genes were cloned from tissues other than testis preclude us from classifying SSTK as a testis-specific kinase. The physiological relevance, if any, of SSTK expression in nontesticular adult tissues is not presently known.

SSTK was found to phosphorylate basic proteins such as MBP, histones H1, H2A, H2AX, and H3, and itself. Our studies using synthetic peptides demonstrated that SSTK prefers to phosphorylate Ser residues with an Arg at the −3 position. However, the peptide substrate data indicated that Arg at −3 was not obligatory for efficient catalysis. Nevertheless, SSTK

evaluation of SSTK expression in testes from wild-type (a and c) and *SSTK* null (b and d) mice. The *SSTK* mRNA was detected (green) in fibromyocytes of the lamina propria (far upper left) and in elongating spermatids (far middle left) of seminiferous tubules of the wild type (a). In situ sections were counterstained with propidium iodide (a and b, red). Immunohistochemical positivity was detected in the heads of elongating spermatids (c and far lower left, brown), and sections were counterstained with hematoxylin.

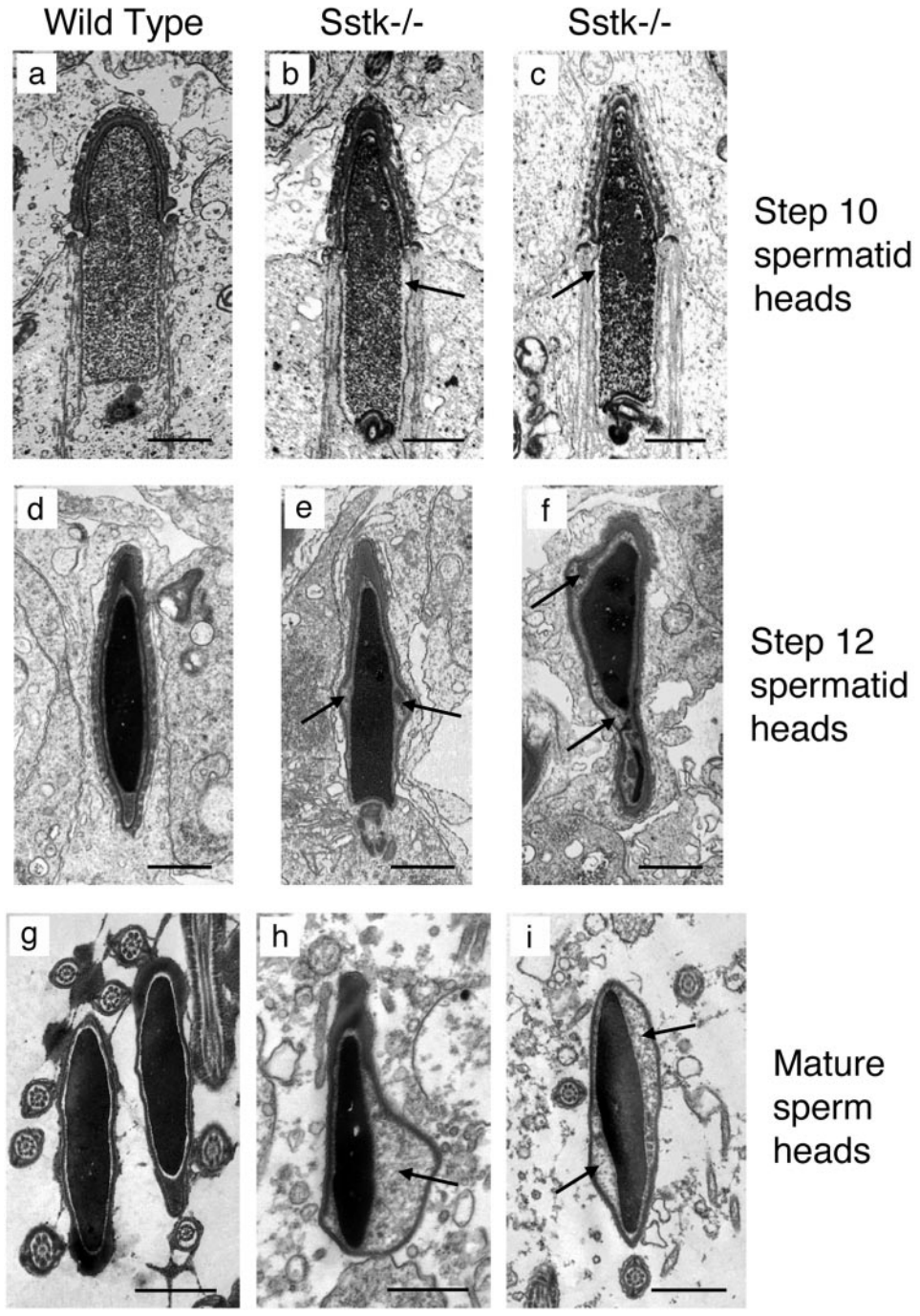

FIG. 6. Electron micrographs of elongating spermatid and mature spermatozoal heads from wild-type and SSTK null mice. Expanded perinuclear and subacrosomal space and accumulation of electron-dense substance are indicated with arrows. Bar, 1 μm.

appears to have a substrate specificity similar to that of other members of the CaMK family, namely, a preference for an R/K-X-X-S/T motif (29).

SSTK associates with heat shock proteins. Our results suggest that SSTK is a subunit of a protein heterooligomer which contains the heat shock proteins. SSTK forms specific stable protein complexes with molecular chaperones HSP90-1β, HSC70, and HSP70-1, but these associated heat shock proteins do not serve as substrates for the kinase. In this work, we expressed SSTK in two different mammalian cell lines, and in both cases the enzyme was complexed with heat shock proteins and constitutively active. Myc-SSTK protein expressed in bacteria was not soluble, and we were not able to refold SSTK to make it soluble in aqueous solution. However, a soluble SSTK–glutathione *S*-transferase fusion protein produced in bacteria had no detectable kinase activity (data not shown). Our results suggest that associated heat shock proteins are necessary for SSTK activity.

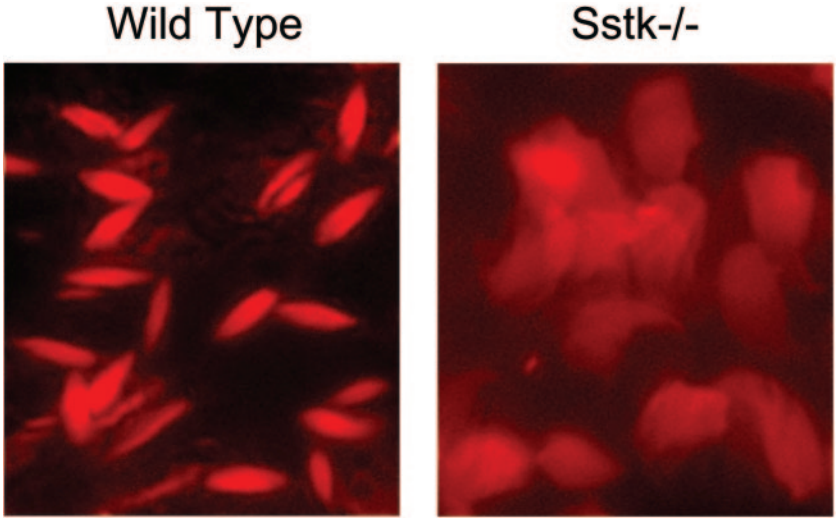

FIG. 7. Fluorescence microscopy evaluation of DNA condensation in the epididymal sperm from wild-type and SSTK knockout mice. Formalin-fixed sections of epididymis were stained with propidium iodide (×1,000).

HSC70 and HSP90-β are constitutively and ubiquitously expressed proteins. Most of HSP90 "client proteins" belong to signal transduction and regulation molecules, including a variety of tyrosine and serine/threonine protein kinases involved in mitogenic signaling and cell cycle regulation, transcription factors, and steroid hormone receptors (reviewed in references 24 and 27). HSP90 acts as a core of a multicomponent chaperone system that may also include HSC70, HSP70, and other proteins (25, 26). It should be noted that HSP90-based molecular chaperone complexes display distinct specificity for kinase binding. For example, HSP90 forms stable complexes with MAP-related protein kinase MOK, male germ cell-associated kinase MAK (both abundantly expressed in the human testis), and MAK-related kinase MRK (abundantly expressed in the human ovary), but does not associate with conventional mitogen-activated kinases ERK, p38, and JNK/SAPK (21). Complex formation with HSP90 and partner proteins HSC70 and HSP70 protects MOK from degradation through proteosome-dependent pathways. Another characteristic example is that HSP90 complexed with cell division cycle 37 homolog Cdc37 binds cyclin-dependent protein kinases Cdk4 and Cdk6 but not Cdk2, Cdk3, Cdk5, or Cdk-activating kinase Cak (reviewed in reference 21). However, we were not able to detect Cdc37 bound to Myc-SSTK, strongly suggesting that Cdc37 is not part of the heat shock protein-SSTK protein complex (data not shown).

Heat shock proteins play an important role in male gametogenesis. In addition to heat shock proteins that are expressed in somatic cells, testis-specific members of the HSP70 family are expressed during spermiogenesis. One of these proteins, spermatocyte-specific HSP70-2, is indispensable for male fertility in mice (6, 7). Interaction of HSP70-2 with Cdc2 is required for Cdc2 complex formation with cyclin B1, Cdc2 kinase activity, and proper germ cell progression through meiosis (35). Another testis-specific chaperone, HSC70t, is expressed in postmeiotic spermatids as they progress from step 9 to the completion of spermatogenesis, but the precise role of this protein is not known (31). In addition to maintaining SSTK structure, heat shock proteins may play a critical role in targeting SSTK to specific subcellular sites.

SSTK is essential for fertility in male mice. Based on immunohistochemistry and in situ hybridization data, we conclude that SSTK belongs to a group of genes that are expressed at late stages of spermiogenesis. This developmental stage involves chromatin condensation, reconstruction of the sperm cytoplasm, acrosome formation, and development of the flagellar apparatus. The mechanisms of postmeiotic chromatin condensation are not well understood. However, phosphorylation events may be important for chromatin compaction and proper DNA packaging. It was shown that newly synthesized protamines and TP2 in the mammalian seminiferous tubules

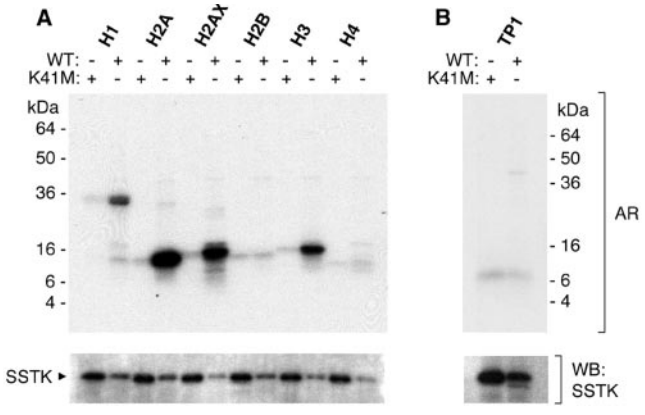

FIG. 8. Phosphorylation of histones by SSTK. Wild-type (WT) and K41M Myc-SSTKs were immunopurified from 32D cells and subjected to in vitro kinase reactions for 30 min at 25°C with [^{32}P]ATP and 0.1 μg/μl of histone H1, H2A, H2AX, H2B, H3, or H4 (A) or 1 μg/μl of transition protein 1 (TP1, B). Reaction mixtures were fractionated in SDS-PAGE gels, transferred to membranes, and autoradiography (AR) was performed for 2.5 h. SSTK antiserum was used in Western blotting (WB). The purity of substrates was confirmed by SDS-PAGE (data not shown).

undergo rapid phosphorylation followed by subsequent partial dephosphorylation (11). Targeted disruption of the catalytic subunit of the protein phosphatase PP1cγ led to impaired meiosis, aberrant retention of histone H3 in step 15 elongated spermatids, and male infertility (32). A protein kinase A-like enzyme activity that phosphorylates TP2 was detected in the nuclear extract from elongated spermatids, and phosphorylation greatly reduced the DNA condensation property of TP2 (19). Unlike somatic cell histones, which have been studied extensively in recent years (2, 10), postmeiotic histone phosphorylation has not been demonstrated, and no specific kinase has been implicated in this process.

Targeted disruption of the *SSTK* gene produced sterility in male mice which was accompanied by reduced sperm numbers, impaired DNA condensation, and abnormal morphology and impaired motility of spermatozoa. Phalloidin staining of seminiferous tubules and epididymis did not reveal any significant differences in the developing germ cells and spermatozoa of SSTK null and wild-type mice (data not shown). These results indicate that the abnormal morphology of SSTK null spermatids and reduced sperm motility were not due to defects in actin cytoskeleton reorganization.

The earliest abnormalities in germ cells from SSTK null males were detected in the heads of step 10 spermatids, coincident with the beginning of histone replacement with transition proteins. Characteristic expansion of the perinuclear and subacrosomal space and accumulation of amorphous electron-dense material between the nuclear envelope and the nucleus indicate abnormal and incomplete chromatin condensation in SSTK-deficient spermatids. Taking into account the localization of SSTK to the heads of spermatids undergoing histone displacement by transition proteins and SSTK's ability to specifically phosphorylate histones H1, H2A, H2AX, and H3, our data indicate that SSTK may be required for proper removal of histones from chromatin in the condensing spermatid nucleus. However, we should note that SSTK was also detected in the fibromyocytes of the seminiferous tubule lamina propria, and we cannot rule out that SSTK in these cells plays a role in male reproduction. Reduced sperm numbers in SSTK null and heterozygous males relative to wild-type mice suggest that SSTK levels may be involved in the control of apoptosis during spermiogenesis. However, sperm numbers were similar in the heterozygous and knockout mice, indicating that enhanced apoptosis cannot be responsible for the infertility phenotype observed.

There are few known protein kinase genes that are indispensable for male fertility. Disruption of the *Camk4* gene results in male sterility, impairment of spermiogenesis, and abnormal sperm heads morphology (34). Similar to SSTK, CaMK4 is involved in postmeiotic chromatin condensation. However, the defect observed in the CaMK4 knockout mice occurs at a later step in spermiogenesis than the defect which we observed in the SSTK null mutants. CaMK4 phosphorylates protamine 2 in vitro, which is thought to be its in vivo substrate. Disruption of the gene encoding the casein kinase 2α′ catalytic subunit affects morphogenesis of the sperm head, resulting in oligozoospermia, abnormal shape of the spermatid nucleus, and extensive germ cell degenerative processes at all stages of spermiogenesis (8). Cdk2, although dispensable for mitosis, is essential for completing meiotic division in mouse germ cells (23). Surprisingly, the male germ cell-associated kinase MAK is dispensable for sperm formation, and targeted deletion led only to a mild reduction in sperm motility and decreased litter sizes (30).

Impairment of sperm chromatin condensation is common in infertile male patients (13, 22). However, the molecular mechanisms underlying these defects remain largely obscure. Identification of SSTK and its role in spermiogenesis may provide insight into the basis of certain human male infertility disorders.

ACKNOWLEDGMENTS

We thank Svetlana Shabalina, Donald Fink, Harold Dickensheets, and Kurt Stromberg for helpful discussions.

REFERENCES

1. **Altschul, S. F., T. L. Madden, A. A. Schaffer, J. Zhang, Z. Zhang, W. Miller, and D. J. Lipman.** 1997. Gapped BLAST and PSI-BLAST: a new generation of protein database search programs. Nucleic Acids Res. **25:**3389–3402.
2. **Ausio, J., D. W. Abbott, X. Wang, and S. C. Moore.** 2001. Histone variants and histone modifications: a structural perspective. Biochem. Cell Biol. **79:** 693–708.
3. **Cobb, M. H., and E. J. Goldsmith.** 1995. How MAP kinases are regulated. J. Biol. Chem. **270:**14843–14846.
4. **Deb, T. B., L. Su, L. Wong, E. Bonvini, A. Wells, M. David, and G. R. Johnson.** 2001. Epidermal growth factor (EGF) receptor kinase-independent signaling by EGF. J. Biol. Chem. **276:**15554–15560.
5. **Deb, T. B., L. Wong, D. S. Salomon, G. Zhou, J. E. Dixon, J. S. Gutkind, S. A. Thompson, and G. R. Johnson.** 1998. A common requirement for the catalytic activity and both SH2 domains of SHP-2 in mitogen-activated protein (MAP) kinase activation by the ErbB family of receptors. A specific role for SHP-2 in map, but not c-Jun amino-terminal kinase activation. J. Biol. Chem. **273:**16643–16646.
6. **Dix, D. J., J. W. Allen, B. W. Collins, C. Mori, N. Nakamura, Poorman-Allen, E. H. P. Goulding, and E. M. Eddy.** 1996. Targeted gene disruption of Hsp70-2 results in failed meiosis, germ cell apoptosis, and male infertility. Proc. Natl. Acad. Sci. USA **93:**3264–3268.
7. **Eddy, E. M.** 1999. Role of heat shock protein HSP70-2 in spermatogenesis. Rev. Reprod. **4:**23–30.
8. **Escalier, D., D. Silvius, and X. Xu.** 2003. Spermatogenesis of mice lacking CK2α′: failure of germ cell survival and characteristic modifications of the spermatid nucleus. Mol. Reprod. Dev. **66:**190–201.
9. **Fan, Y. X., L. Wong, T. B. Deb, and G. R. Johnson.** 2004. Ligand regulates epidermal growth factor receptor kinase specificity: activation increases preference for GAB1 and SHC versus autophosphorylation sites. J. Biol. Chem. **279:**38143–38150.
10. **Green, G. R.** 2001. Phosphorylation of histone variant regions in chromatin: unlocking the linker? Biochem. Cell Biol. **79:**275–287.
11. **Green, G. R., R. Balhorn, D. L. Poccia, and N. B. Hecht.** 1994. Synthesis and processing of mammalian protamines and transition proteins. Mol. Reprod. Dev. **37:**255–263.
12. **Gu, Y., J. Rosenblatt, and D. O. Morgan.** 1992. Cell cycle regulation of CDK2 activity by phosphorylation of Thr160 and Tyr15. EMBO J. **11:**3995–4005.
13. **Hammadeh, M. E., T. Zeginiadov, P. Rosenbaum, T. Georg, W. Schmidt, and E. Strehler.** 2001. Predictive value of sperm chromatin condensation (aniline blue staining) in the assessment of male fertility. Arch. Androl. **46:**99–104.
14. **Hanks, S., and T. Hunter.** 1995. The eukaryotic protein kinase superfamily: kinase (catalytic) domain structure and classification. FASEB J. **9:**576–596.
15. **Hardie, D. G.** 2000. Metabolic control: a new solution to an old problem. Curr. Biol. **10:**R757–759.
16. **Hunter, T.** 2000. Signaling—2000 and beyond. Cell **100:**113–127.
17. **Hunter, T. R., and B. M. Sefton.** 1980. Transforming gene product of Rous sarcoma virus phosphorylates tyrosine. Proc. Natl. Acad. Sci. USA **77:**1311–1315.
18. **Huse, M., and J. Kuriyan.** 2002. The conformational plasticity of protein kinases. Cell **109:**275–282.
19. **Meetei, A. R., K. S. Ullas, V. Vasupradha, and M. R. Rao.** 2002. Involvement of protein kinase A in the phosphorylation of spermatidal protein TP2 and its effect on DNA condensation. Biochemistry **41:**185–195.
20. **Meistrich, M. L., B. Mohapatra, C. R. Shirley, and M. Zhao.** 2003. Roles of transition nuclear proteins in spermiogenesis. Chromosoma **111:**483–488.
21. **Miyata, Y., Y. Ikawa, M. Shibuya, and E. Nishida.** 2001. Specific association of a set of molecular chaperones including HSP90 and Cdc37 with MOK, a member of the mitogen-activated protein kinase superfamily. J. Biol. Chem. **276:**21841–21848.

22. **Molina, J., J. A. Castilla, J. L. Castano, J. Fontes, N. Mendoza, and L. Martinez.** 2001. Chromatin status in human ejaculated spermatozoa from infertile patients and relationship to seminal parameters. Hum. Reprod. **16:** 534–539.
23. **Ortega, S., I. Prieto, J. Odajima, A. Martin, P. Dubus, R. Sotillo, J. L. Barbero, M. Malumbres, and M. Barbacid.** 2003. Cyclin-dependent kinase 2 is essential for meiosis but not for mitotic cell division in mice. Nat. Genet. **35:**25–31.
24. **Picard, D.** 2002. Heat-shock protein 90, a chaperone for folding and regulation. Cell. Mol. Life Sci. **59:**1640–1648.
25. **Polanowska-Grabowska, R., and A. R. Gear.** 2000. Heat-shock proteins and platelet function. Platelets **11:**6–22.
26. **Pratt, W. B., and D. O. Toft.** 2003. Regulation of signaling protein function and trafficking by the hsp90/hsp70-based chaperone machinery. Exp. Biol. Med. **228:**111–133.
27. **Richter, K., and J. Buchner.** 2001. Hsp90: chaperoning signal transduction. J. Cell. Physiol. **188:**281–290.
28. **Sassone-Corsi, P.** 2002. Unique chromatin remodeling and transcriptional regulation in spermatogenesis. Science **296:**2176–2178.
29. **Seo, G. J., S. E. Kim, Y. M. Lee, J. W. Lee, J. R. Lee, M. J. Hahn, and S. T. Kim.** 2003. Determination of substrate specificity and putative substrates of Chk2 kinase. Biochem. Biophys. Res. Commun. **304:**339–343.
30. **Shinkai, Y., H. Satoh, N. Takeda, M. Fukuda, E. Chiba, T. Kato, T. Kuramochi, and Y. Araki.** 2002. A testicular germ cell-associated serine-threonine kinase, MAK, is dispensable for sperm formation. Mol. Cell. Biol. **22:**3276–3280.
31. **Tsunekawa, N., M. Matsumoto, S. Tone, T. Nishida, and H. Fujimoto.** 1999. The Hsp70 homolog gene, Hsc70t, is expressed under translational control during mouse spermiogenesis. Mol. Reprod. Dev. **52:**383–391.
32. **Varmuza, S., A. Jurisicova, K. Okano, J. Hudson, K. Boekelheide, and E. B. Shipp.** 1999. Spermiogenesis is impaired in mice bearing a targeted mutation in the protein phosphatase 1cγ gene. Dev. Biol. **205:**98–110.
33. **Wilm, M., A. Shevchenko, T. Houthaeve, S. Breit, L. Schweigerer, T. Fotsis, and M. Mann.** 1996. Femtomole sequencing of proteins from polyacrylamide gels by nano-electrospray mass spectrometry. Nature **379:**466–469.
34. **Wu, J. Y., T. J. Ribar, D. E. Cummings, K. A. Burton, G. S. McKnight, and A. R. Means.** 2000. Spermiogenesis and exchange of basic nuclear proteins are impaired in male germ cells lacking Camk4. Nat. Genet. **25:**448–452.
35. **Zhu, D., D. J. Dix, and E. M. Eddy.** 1997. HSP70-2 is required for CDC2 kinase activity in meiosis I of mouse spermatocytes. Development **124:**3007–3014.